Supplementary Information

UPLC-MS/MS investigation of β-glucan oligosaccharide oxidation

Samy Boulos and Laura Nyström*

ETH Zurich, Institute of Food, Nutrition and Health – Schmelzbergstrasse 9, 8092 Zurich, Switzerland.

*Corresponding author. Phone: +41 44 632 91 65. Email: laura.nystroem@hest.ethz.ch.

Contents

1. UPLC-MS/MS method: additional information

Injection: The Glc_4 degradation samples were analysed directly as neat reaction mixtures (2.5 µL injection volume), after catalase treatment (2.5 µL), and/or after dilution (to 75% ACN; 10 µL). For the longer gradient 2 (0.1% NH_3) and gradient 3 (60 mM NH_4HCO_2, pH 8), the sample was always injected after dilution (75% ACN) with and without prior catalase treatment. For the short gradient 1, where solvent effects play a negligible role, the samples were also injected undiluted.[i]

MS conditions: The spectra were generally acquired in resolution mode, apart from the high resolution measurements for Table 1 in the paper (note that products with $\Delta m \geq 0.03$ Da are also distinguishable already in resolution mode on the Synapt G2 qToF instrument, and were confirmed by high resolution mode measurements). Two sets of voltages were used for the sample cone and extraction cone, named hereafter

ESI-method A: 25 and 4 V, respectively, and

ESI-method B: 15 and 3 V, respectively.

Table S1 Collision energy (CE) ramps for MS/MS of native oligosaccharides and their oxidation products.

m/z	Trap CE [V]	Transfer CE [V]
679.19	-	10-30
665.21	-	5-25
663.20	-	5-15
635.20	-	5-15
605.19	-	5-15
519.16	-	15-25
517.14	-	10-25
503.16	-	5-10
501.15	-	5-10
473.15	-	5-10
443.14	-	5-10
357.10	-	10-15
355.09	-	5-15
683.23[a]	10	5-15

[a] Glc_2 ionized as its dimer $[2Glc_2 - H]^-$.

[i] Catalase-treated aliquots served as control to compare with injections made with non-treated samples to ensure that H_2O_2 on the column as well as freezing and storage of neat and diluted reaction mixtures had no significant effect on the observed product profiles if analysed immediately after thawing. Catalase treatment also allowed repeated analysis of the aliquots over prolonged periods of time (autosampler at 4 °C) without progressing degradation, but led to additional artefact peaks from the buffer and catalase material (marked in the respective chromatograms; confirmed by injecting diluted catalase buffer solution).

2. Kinetics of the degradation

Mechanistically, the degradation of Glc_4 model compounds includes three relevant reactions with their respective rate laws of second order kinetics shown below: (i) the Fenton-reaction for $HO^{\bullet}$-production, (ii) the reaction of $HO^{\bullet}$ with Glc_4, and (iii) the reduction of Fe(III) formed in the Fenton-reaction back to Fe(II) to close the catalytic cycle (e.g. by ascorbic acid, $O_2^{\bullet-}$):

	Reaction	**Second order rate law**
(i)	$Fe^{2+} + H_2O_2 \rightarrow Fe^{3+} + OH^- + HO^{\bullet}$	$d[HO^{\bullet}]/dt = k_{Fenton} \cdot [Fe^{2+}] \cdot [H_2O_2]$
(ii)	$Glc_4\text{–}H + HO^{\bullet} \rightarrow Glc_4^{\bullet} + H_2O$	$-d[Glc_4]/dt = k_{Glc4} \cdot [HO^{\bullet}] \cdot [Glc_4]$
(iii)	Fe^{3+} + reductant $\rightarrow$ Fe^{2+} + (oxidized reductant)	$d[Fe^{2+}]/dt = k_{red} \cdot [Fe^{3+}] \cdot [\text{reductant}]$

The investigated Glc_4 degradation system (1 mM Glc_4, 50 µM $FeSO_4$, 50 µM AA, 10 mM H_2O_2) followed a pseudo first order kinetic behaviour (see Fig. S6), which means that $HO^{\bullet}$ remained at a constant steady state concentration $[HO^{\bullet}]_{ss}$, effectively making the observed rate law:

$$-d[Glc_4]/dt = k_{obs} \cdot [Glc_4] \qquad \text{with } k_{obs} = k_{Glc4} \cdot [HO^{\bullet}]_{ss},$$

explaining the exponential decay observed in Fig. S6.

Rational behind negligible secondary oxidation occurring at low substrate conversion

The reaction rate ratios of oxidative attack by $HO^{\bullet}$ on Glc_4 and on a primary oxidation product P is

$-d[Glc_4]/dt : -d[P]/dt = k_{Glc4}[HO^{\bullet}][Glc_4] : k_P[OH][P]$

and thus, assuming equal rate constants $k_{Glc4} \approx k_P$ for the abstraction of a hydrogen atom by $HO^{\bullet}$, the rate ratios are

$-d[Glc_4]/dt : -d[P]/dt \approx [Glc_4]/[P]$.

Due to the smaller size of the products (less glucose units) compared to the starting material, the rate constant of the $HO^{\bullet}$-attack k_P is most likely smaller than k_{Glc4}, pushing the relative rate ratio even more in favour of Glc_4. It follows that at low conversion where $[Glc_4] >> [P]$, the rates must also be $-d[Glc_4]/dt >> -d[P]/dt$, meaning negligible secondary oxidation. This is contrary to the experimental observation for the *m*/*z* 193, 355, 517 products, which cannot be formed by less than two oxidative attacks and thus necessarily represent secondary products (3 h MS in Fig. 3).

3. Ratios of primary and secondary oxidation products

Two sets of calculations were made with classification of the acidic oxidation products from Fenton-induced Glc_4 oxidation into primary and secondary oxidation products using different kinds of averages.[ii] The gluconic acid bearing oligomers $Glc_{(n-1)}Glc1A$ with *m*/*z* 195.05, 357.10, 519.16, and 681.21 for n = 1, 2, 3, and 4, respectively, were assumed to be primary oxidation products. The first secondary oxidation products were assumed to be the respective *m*/*z* with − 2 Da, namely *m*/*z* 193.04, 355.09, 517.14, and 679.19. "All secondary oxidation products" includes the respective *m*/*z* with − 2 Da, − 4 Da, and − 6 Da, corresponding to gluconic acid bearing oligomers with one, two, or three additional carbonyl groups, respectively.

The first set of calculations (Fig. S7a in the paper) looked at the MS signal ratios of secondary oxidation products to primary oxidation products as a function of oxidation time t, while taking the average of all oligomer species of all sizes n for each time point:

$$ratio(t) = \frac{1}{4}\sum_{n=1}^{4}\frac{signal(1st\ secondary(n,t))}{signal(primary(n,t))} \quad \text{(S1)}$$

$$ratio(t) = \frac{1}{4}\sum_{n=1}^{4}\frac{\sum signal(all\ secondary(n,t))}{signal(primary(n,t))} \quad \text{(S2)}$$

The second set of calculations (Fig. S7b) looked at the MS signal ratios of secondary oxidation products to primary oxidation products as a function of total sugar units n, while taking the average of the respective products over the whole oxidation time:

$$ratio(n) = \frac{1}{5}\sum_{t=3h}^{72h}\frac{signal(1st\ secondary(n,t))}{signal(primary(n,t))} \quad \text{(S3)}$$

$$ratio(n) = \frac{1}{5}\sum_{t=3h}^{72h}\frac{\sum signal(all\ secondary(n,t))}{signal(primary(n,t))} \quad \text{(S4)}$$

The error bars in the graphs (Fig. S7) are the respective normalized standard deviations of the averages.

[ii] Note that in the case of $Glc_{(n-1)}GlcUA$, only n = 1, 2, 3 are secondary oxidation products, whereas for isobaric oxo-$Glc_{(n-1)}Glc1A$, all n = 1 – 4 need two oxidative steps.

4. Spectral similarity score

In order to identify which oligomer led to which gluconic acid products, spectral similarity scores as described by Mulroney *et al.* for disaccharide MS/MS were calculated according to the following formula:[iii]

$$similarity = \frac{\sum \sqrt{I_m^1 I_m^2}}{\sqrt{\left(\sum I_m^1\right)\left(\sum I_m^2\right)}} \quad \text{(S5)}$$

with I^1_m and I^2_m being intensities of an ion at $m/z = m$ for the two spectra. The most diagnostic set of fragment ions were selected for the calculation (see Table S2). This was especially of value for the mixed-linkage glucotrionic acids that co-eluted also using UPLC gradient 3 (buffered ammonium formate eluent). This and the fact that gluconic acid bearing oligomers have a lower MS/MS fragmentation yield compared to neutral oligomers, thus being prone to sensitivity problems and to spectral contaminations by co-eluting in-source fragmenting products, made spectral similarity score calculations a valuable tool to assess those products and allowed identifying the major component nonetheless.

Table S2 Diagnostic set of MS/MS fragmentation ions of glucobionic (*m/z* 357.10) and glucotrionic acids (*m/z* 519.16) used for spectral similarity score calculations.

Glucobionic acids m/z	Glucotrionic acids m/z
71.01	75.01
75.01	87.01
85.03	101.02
87.01	113.02
89.02	177.04
141.02	179.06
143.04	221.07
177.04	263.08
179.06	323.10
195.05	383.12
221.07	501.15
339.09	

[iii] B. Mulroney, J. C. Traeger and B. A. Stone, "*Determination of Both Linkage Position and Anomeric Configuration in Underivatized Glucopyranosyl Disaccharides by Electrospray Mass Spectrometry*". *J. Mass Spectrom*., 1995, **30**, 1277-1283.

Table S3 shows the results of both the C1-oxidized standards against one another on the left (prepared by selective oxidation of the reducing end by hypoiodite), as well as the glucobionic and glucotrionic acid oxidation products detected in the various isomeric Glc_4 degradation mixtures. Thereby, the spectral similarity score is always ≤ 1, with 1 meaning full overlap of the two compared spectra. The isomeric gluconic acid standards were distinguishable, giving a non-matching value between 0.560–0.781 (Table S3; left-hand side). Comparison of the similarity scores derived from the Fenton-degraded Glc_4 products and the gluconic acid standards revealed a pattern, whereby one of the scores for each Glc_4 isomer was clearly higher than the others and close to unity (Table S3; right-hand side, marked with *). This indicates that each Glc_4 isomer preferentially reacted to one certain glucobionic and one glucotrionic acid isomer in the Fenton-induced degradation (see Fig. S10 and S11 for spectra).

Table S3 MS/MS spectral similarity scores of gluconic acid standards and detected glucobionic and glucotrionic acid products from the various Fenton-degraded glucotetraose samples after 24 h reaction time.

	Gluconic acid standards			**Native glucotetraoses subjected to Fenton's reagent[a]**			
Structure	G_1-^4G_A	G_1-$^4G_1$-^4G_A	G_1-$^3G_1$-^4G_A	G_1-$^4G_1$-$^4G_1$-$^4\underline{G}$	G_1-$^3G_1$-$^4G_1$-$^4\underline{G}$	G_1-$^4G_1$-$^3G_1$-$^4\underline{G}$	G_1-$^4G_1$-$^4G_1$-$^3\underline{G}$
Glucobionic acid standards				Glucobionic acid products			
G_1-^4G_A	1.000	-	-	0.998*	0.880	0.992*	0.991*
G_1-^3G_A	0.637	-	-	0.626	0.913*	0.695	0.695
Glucotrionic acid standards				Glucotrionic acid products			
G_1-$^4G_1$-^4G_A	-	1.000	-	0.997*	0.855	0.833	0.989*
G_1-$^3G_1$-^4G_A	-	0.781	1.000	0.788	0.941*	0.717	0.791
G_1-$^4G_1$-^3G_A	-	0.767	0.560	0.763	0.780	0.977*	0.836

[a] The highest glucobionic and glucotrionic acid scores of each Glc_4 isomer is marked with an asterisk.

5. Additional chromatograms, MS and MS/MS data

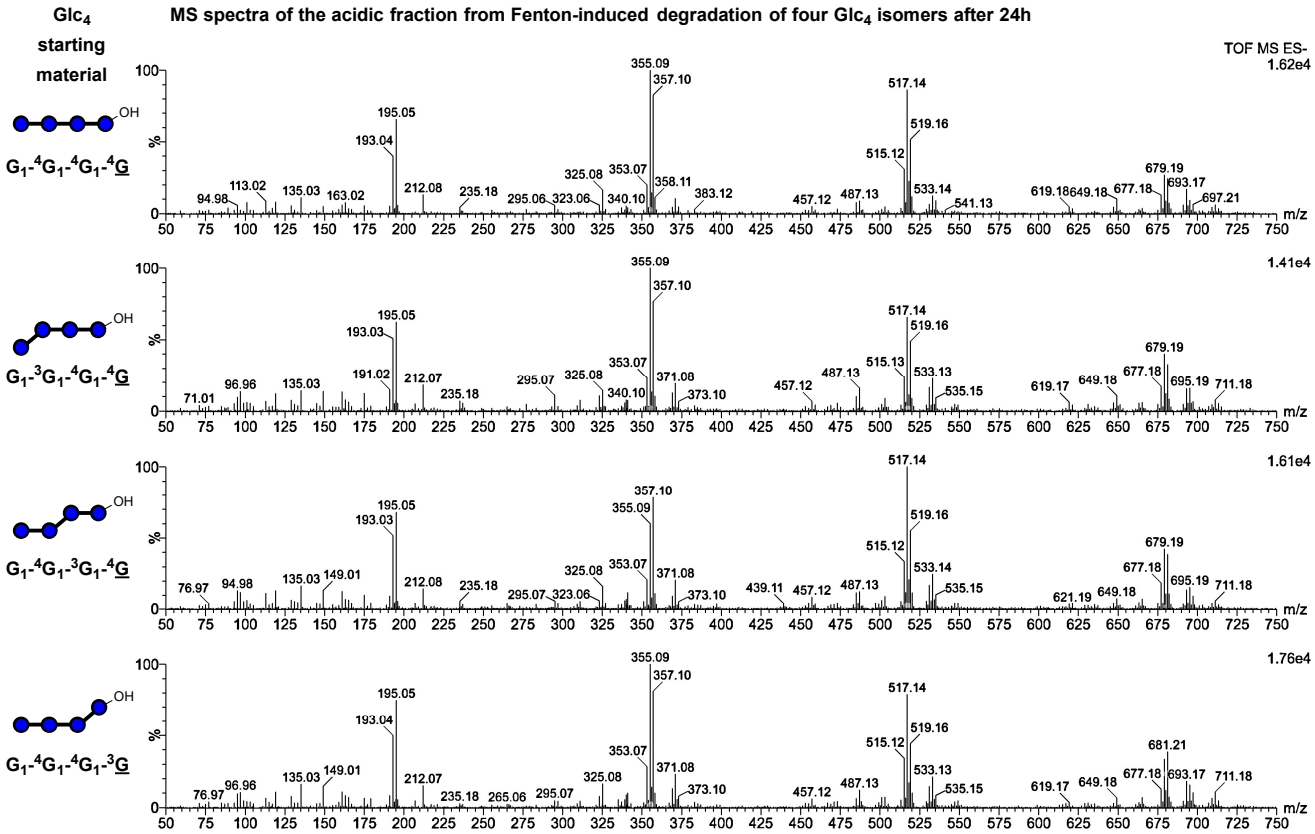

Fig. S1 Collective ESI-MS spectra (negative ion mode) of the acidic products fraction (eluting around 1–2 min) from Glc_4 Fenton-induced oxidation with all four isomers as substrates after 24 h oxidation time. UPLC gradient 1 and ESI-method A were used.

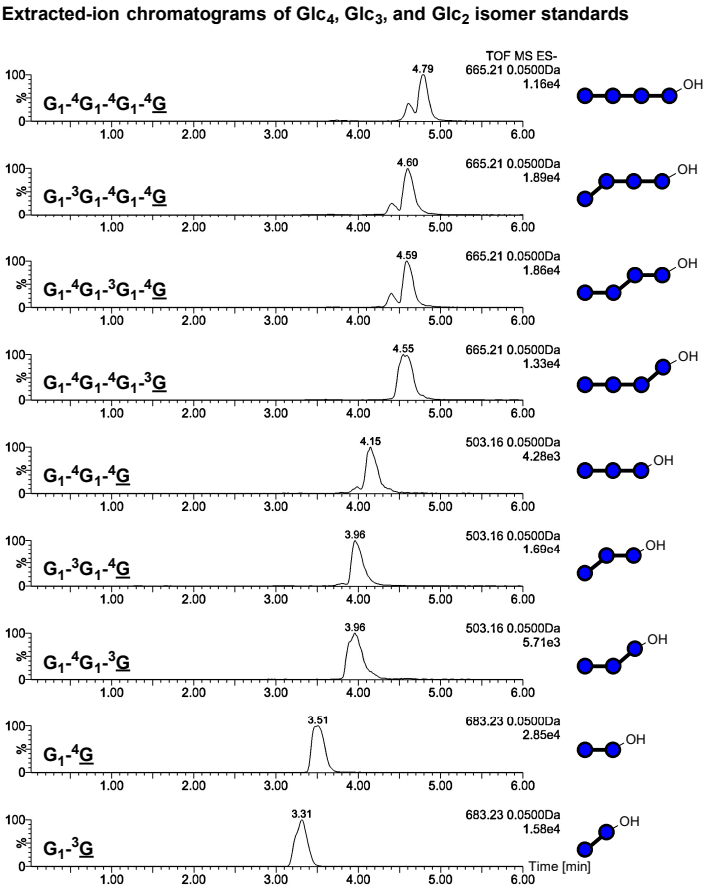

Fig. S2 UPLC-MS extracted-ion chromatograms of Glc_n (n = 2, 3, 4) isomer standards with indicated retention time in minutes (above peak), structure, and m/z of the detected deprotonated species on the right (with the exception of Glc_2 isomers, which ionized as $[2M - H]^-$ = m/z 683.23), analysed using a HILIC BEH Amide column and ACN/H_2O gradient 1 with NH_3 additive (ESI-method A).[iv]

[iv] Note that under the chosen chromatographic conditions, double peaks (or broad peaks) are observed for some of the oligomers (e.g. cellotetraose), which can be attributed to α/β-anomers of the reducing end unit. The basic eluent at 35 °C did apparently not suffice in those cases for accelerated on-column interconversion and coalescence of the two forms. Higher column temperatures were avoided to minimize potential on-column degradation of oxidation products.

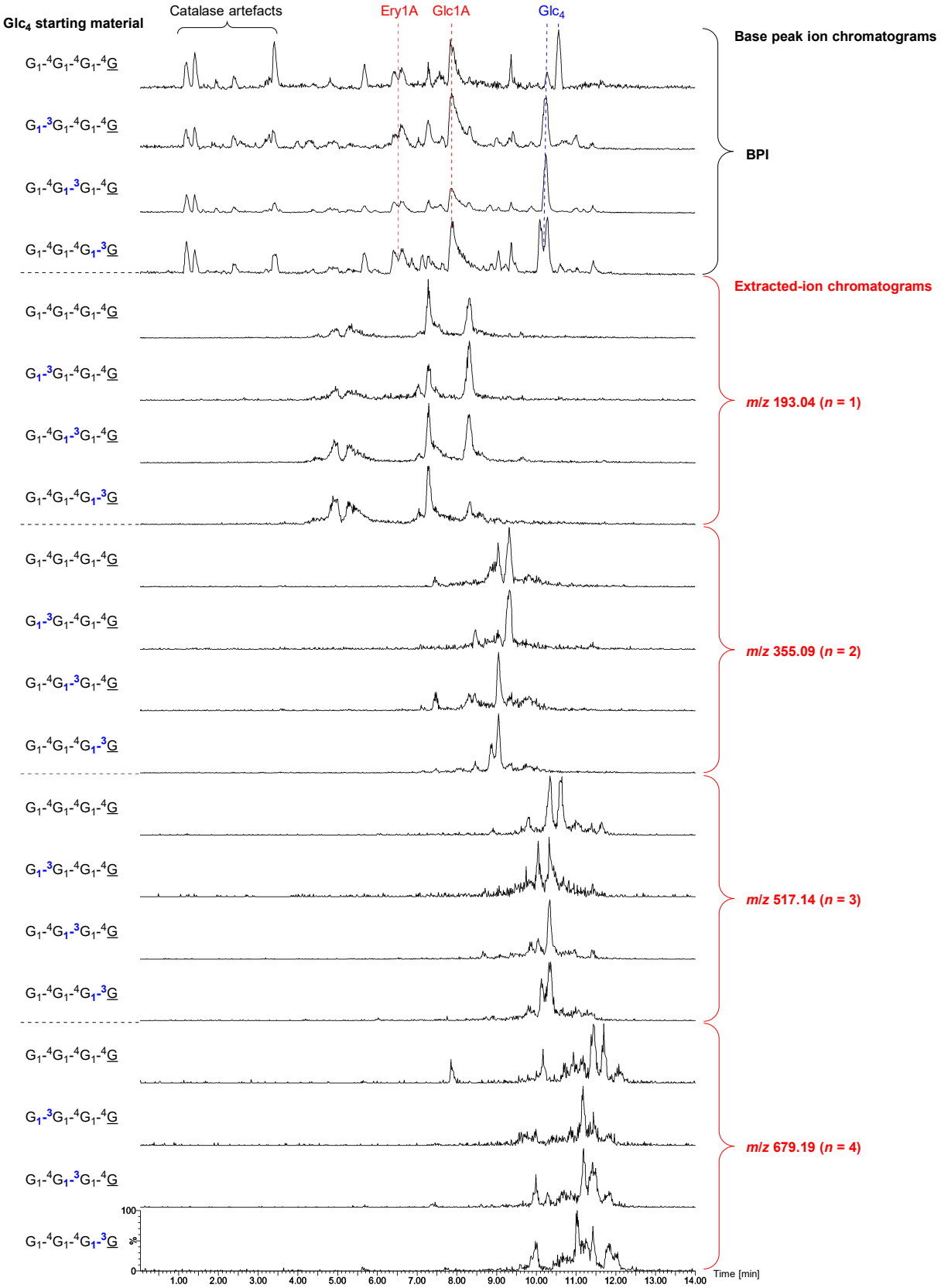

Fig. S3 UPLC-MS base peak ion chromatograms (BPI, top four) and extracted-ion chromatograms of the *m*/*z* 193, 355, 517, 679 series that is presumed to be a mixture of $Glc_{(n-1)}GlcUA$ with the glucuronic acid being anywhere along the oligomer chain, and/or oxo-$Glc_{(n-1)}Glc1A$ (gluconic acid oligomers with an additional carbonyl group) from degradation of four Glc_4 isomers. HILIC BEH Amide column, gradient 3 (60 mM NH_4HCO_2 pH 8 in ACN/H_2O), and ESI-method A were used.

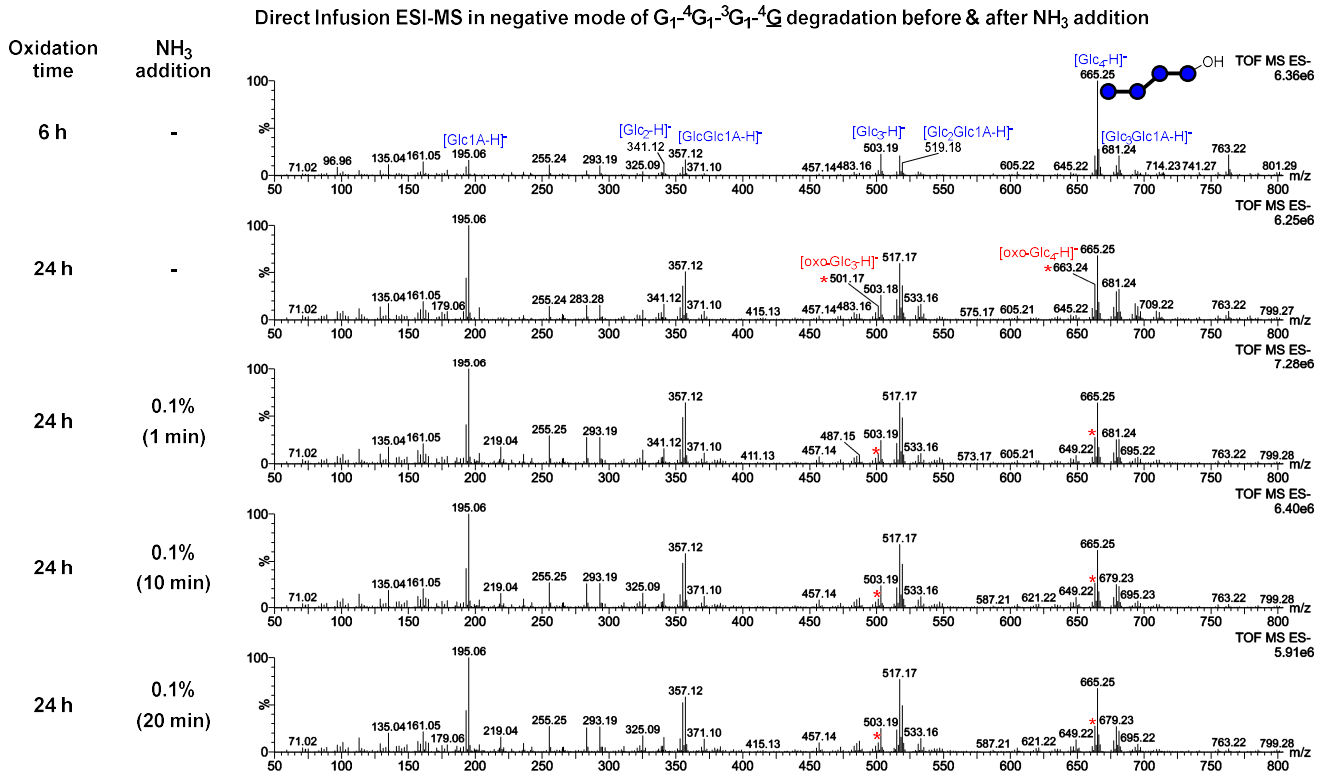

Fig. S4 Control experiment to elucidate potential on-column degradation of oxo-Glc$_n$ products (*) due to basic eluent: Direct infusion ESI-MS in negative ion mode of a 1 mM G1-^{4}G1-^{3}G1-^{4}G solution treated with 50 µM $FeSO_4$, 50 µM AA and 10 mM H_2O_2 after 6 and 24 h reaction time at room temperature (diluted to 75% ACN prior to infusion with 10 µL/min flow rate, ~30 s accumulated signal with 1 Hz scan rate) before and after addition of NH_3. The indicated times in brackets below the NH_3 concentration indicate the incubation time before direct infusion. ESI-method A was used (no lockmass correction).

Table S4 Negative ion MS signal abundance (relative to base peak ion) from direct infusion experiments of starting material (*m/z* 665), Glc$_n$ depolymerization products (*m/z* 503, 341, 179 for *n* = 3, 2, 1, respectively), and oxo-Glc$_n$ products (*m/z* 663 and 501 for *n* = 4 and 3, respectively) at 24 h oxidation time before and after NH_3 addition.[a]

			Signal relative to base peak ion of MS spectrum						Relative to signal before NH_3 addition[b]	
Oxidation time	NH_3 addition	Incubation time	Glc$_4$ *m/z* 665	Glc$_3$ *m/z* 503	Glc$_2$ *m/z* 341	Glc *m/z* 179	oxo-Glc$_4$ *m/z* 663	oxo-Glc$_3$ *m/z* 501	oxo-Glc$_4$ *m/z* 663	oxo-Glc$_3$ *m/z* 501
24 h	-	-	69%	26%	16%	8%	38%	13%	**100%**	**100%**
24 h	0.1%	1 min	64%	24%	15%	7%	27%	10%	**79%**	**79%**
24 h	0.1%	10 min	62%	23%	14%	7%	26%	9%	**76%**	**73%**
24 h	0.1%	20 min	67%	25%	15%	7%	27%	10%	**73%**	**73%**

[a] Extracted from MS spectra shown in Fig. S4. [b] Normalized by first dividing the oxo-Glc$_n$ signal abundance by the respective *m/z* 665 signal for each MS spectrum to compensate for signal fluctuations of neutral oligomers. Note that the sudden drop of oxo-Glc$_n$ signal after NH_3 addition could also be – apart from a different influence on ionization efficiency of Glc$_n$ vs. oxo-Glc$_n$ species – due to contributions of isobaric gluconolactones to the signals that are hydrolysed to the respective gluconic acids (*m/z* 681 and 519 for *n* = 4 and 3, respectively) after NH_3 addition. Hence, the determined drop in signal by ~¼ can be seen as the maximum potential degree of oxo-Glc$_n$ degradation due to NH_3 that may occur on-column during UPLC-MS.

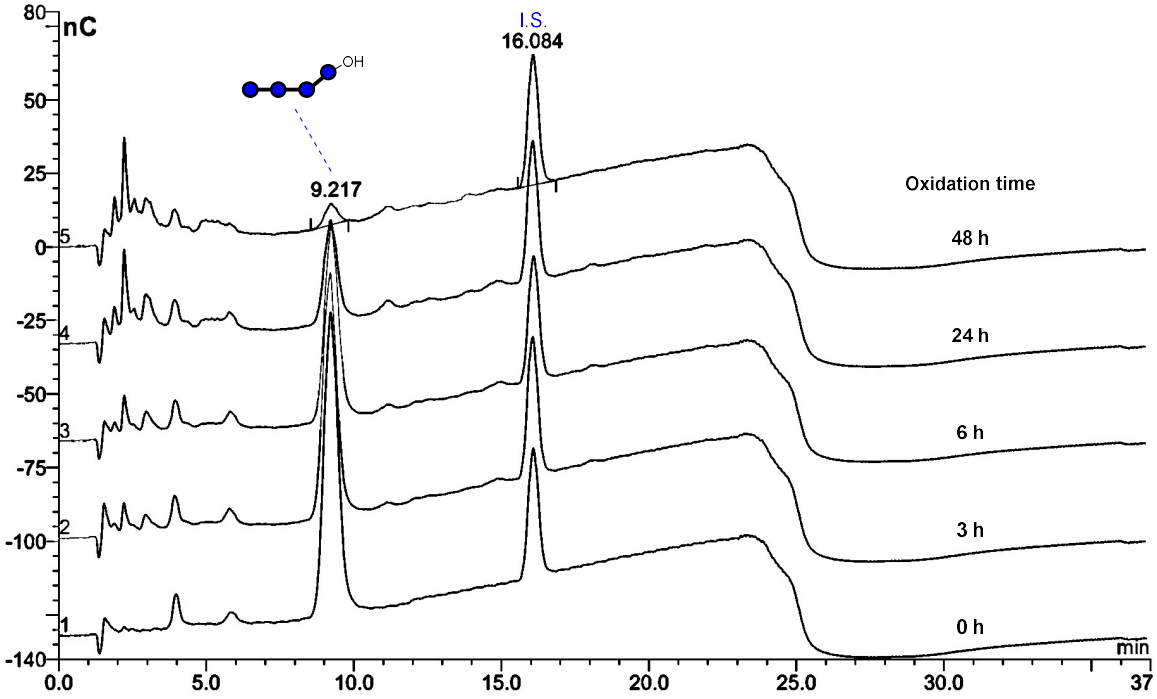

Fig. S5 Examples of HPAEC-PAD chromatograms (analytical Dionex CarboPac PA1 column; 0.15 M NaOH/ 0.5 M NaOAc eluents) taken from the reaction mixture of 1 mM G_1-$^4G_1$-$^4G_1$-$^3\underline{G}$ solution treated with 50 µM $FeSO_4$, 50 µM AA and 10 mM H_2O_2 after 0, 3, 6, 24, and 48 h oxidation time. Remaining starting material (eluting at 9.217 min) was quantified by this method for the degradation kinetics. Note that product formation is mostly seen as peaks eluting before 5 min, in accordance with on-column degradation of oxo-products to smaller oligomers. Later eluting, presumably acidic products appear due to the large number of products (~100 species, Table 1) as "bumby baseline". I.S. = internal standard (maltopentaose).

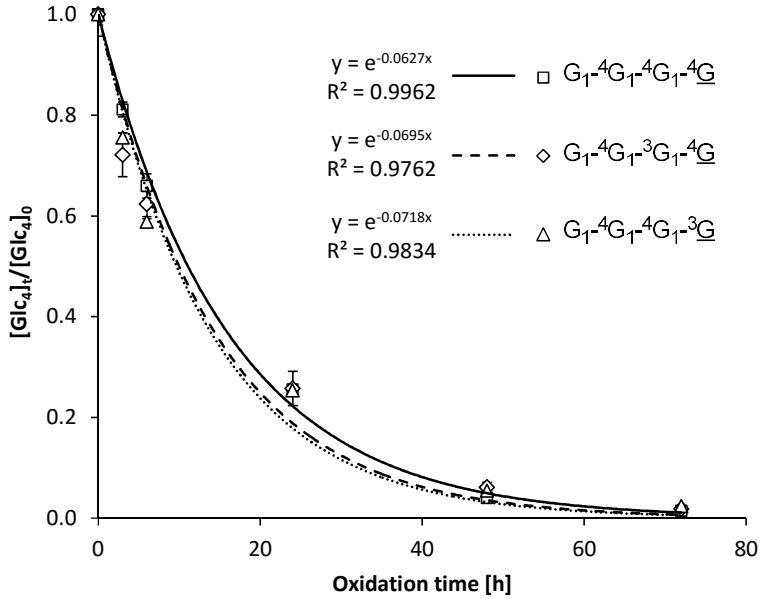

Fig. S6 Oxidation of three isomeric Glc_4 (1 mM) by the Fenton reagents (10 mM H_2O_2, 50 µM $FeSO_4$, 50 µM AA): substrate consumption over time and fitted apparent first order kinetics (quant. by HPAEC-PAD). The standard deviations are shown as error bars. No significant difference was found between the isomers (average $t_{½}$ ~10 h).

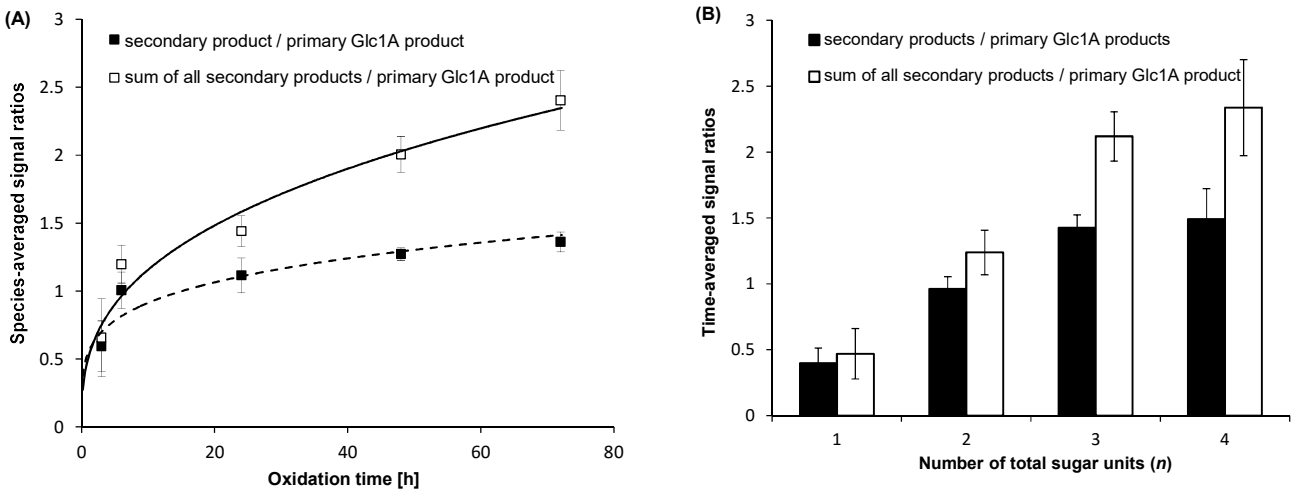

Fig. S7 Fenton-induced degradation of cellotetraose: (A) Species-averaged ratios of secondary oxidation (oxo-Glc$_{(n-1)}$Glc1A & GlcUAGlc$_{(n-1)}$) to primary Glc$_{(n-1)}$Glc1A products over time (equations S1 and S2). Such an increase over time (or in radiolysis: with higher doses) is a general feature of secondary oxidation processes.[v] (B) Time-averaged ratios of secondary oxidation to primary gluconic acid products as a function of the number of total sugar units (equations S3 and S4). The positive correlation of the ratio with the number of total sugar units can be explained by the secondary reactions, which are faster with larger oligomers due to more possible attack sites, leading to a higher probability of attack by HO•.

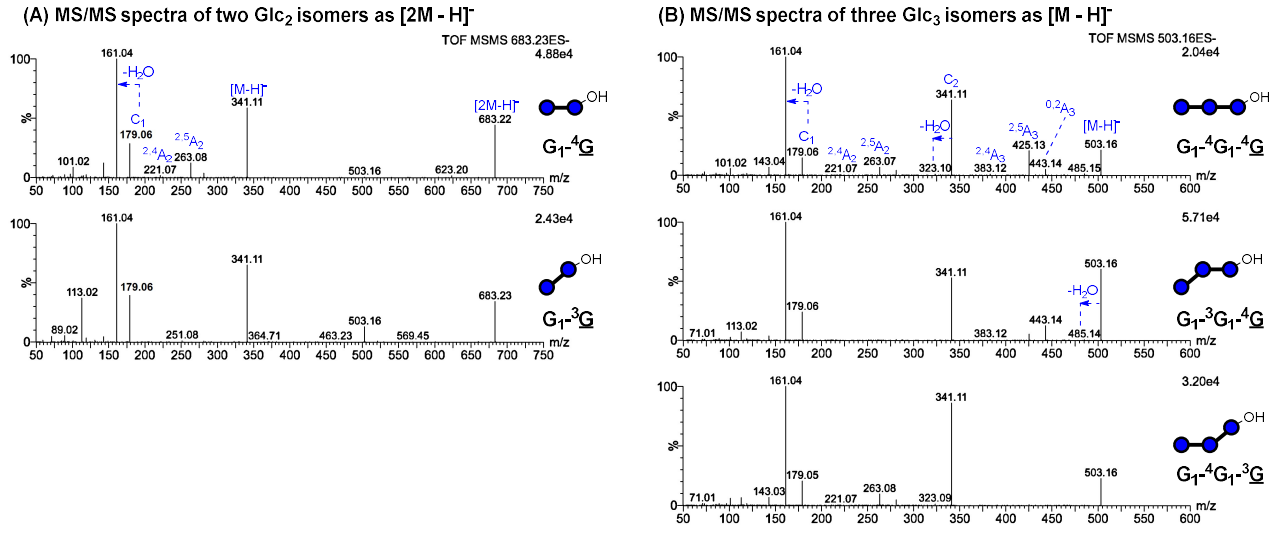

Fig. S8 MS/MS spectra of neutral oligomer standards: (A) Glc$_2$ isomers cellobiose (G$_1$-^{4}G) and laminaribiose (G$_1$-^{3}G) ionized as deprotonated dimers, as well as (B) three Glc$_3$ isomers. ESI-method A was used.

[v] See Fig. 2 & Fig. 3 in: M. N. Schuchmann and C. V. Sonntag, "*Radiation-Chemistry of Carbohydrates 14: Hydroxyl Radical Induced Oxidation of D-Glucose in Oxygenated Aqueous-Solution*". *J. Chem. Soc. Perk. T. 2*, 1977, 1958-1963.

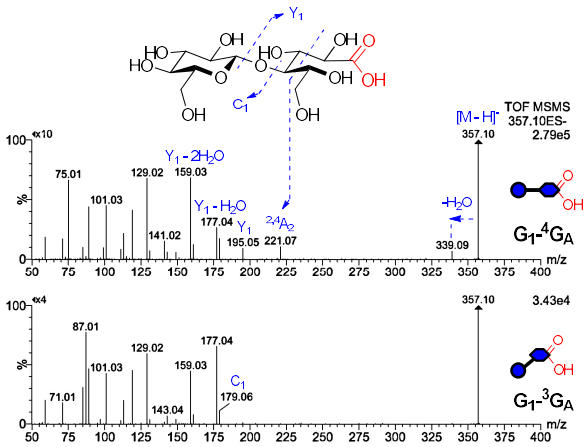

Fig. S9 MS/MS spectra of two glucobionic acid oxidation product standards (*m/z* 357; GlcGlc1A) produced by selective C1-oxidation. The chemical structure corresponds to the top spectrum of cellobionic acid. ESI-method A.

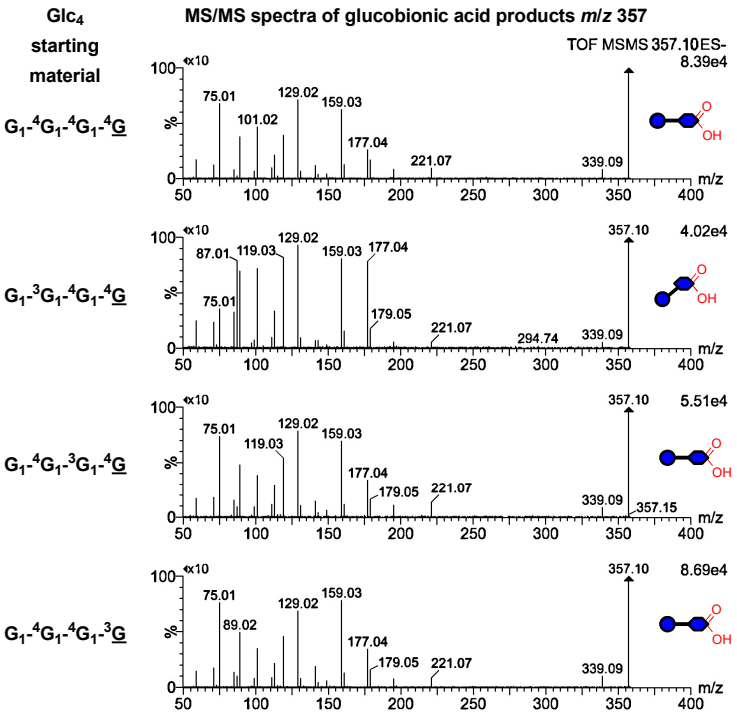

Fig. S10 MS/MS spectra of glucobionic acid products *m/z* 357 (GlcGlc1A) obtained from the various Glc_4 isomers under the Fenton conditions. The depicted product structures refer to the main product isomer as determined by spectral similarity score calculations (equation S5, Table S3). ESI-method A was used.

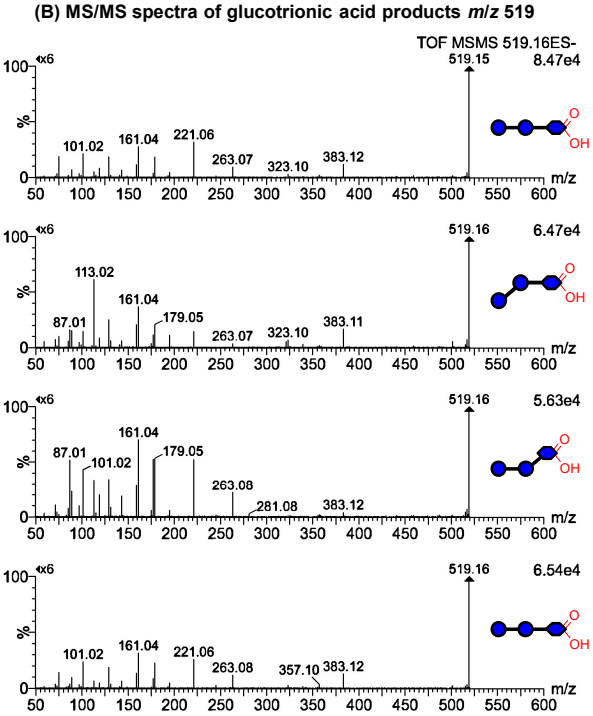

Fig. S11 MS/MS spectra of glucotrionic acid products *m/z* 519 (Glc_2Glc1A) obtained from the various Glc_4 isomers under the Fenton conditions as in Fig. S10.

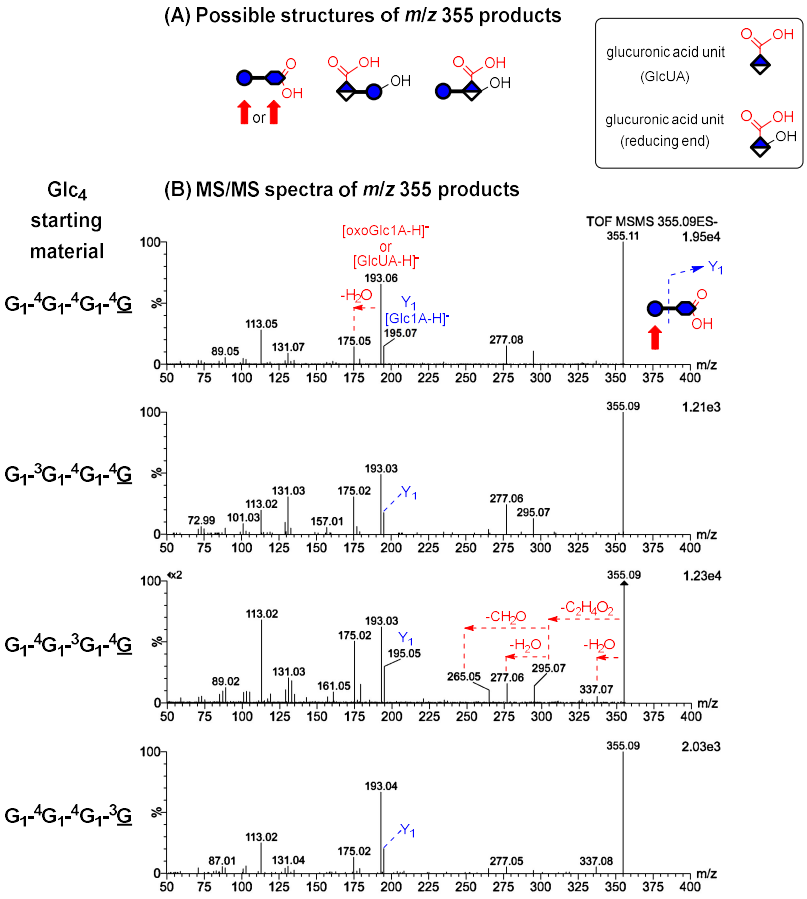

Fig. S12 (A) Possible acidic product structures with *m/z* 355 (oxoGlcGlc1A and GlcGlcUA) shown in the case of cello-oligomers as example. The bold red arrows indicate possible positions of the carbonyl function on the oligomer with presumed gluconic acid end group. (B) Collective MS/MS spectra of *m/z* 355 products obtained from the various Glc_4 isomers under the Fenton conditions. Labelled Y_n fragments (blue) correspond to ions containing the gluconic acid unit, but not the additional carbonyl group, whereas neutral losses in red indicate oxo-product ions. ESI-method A.

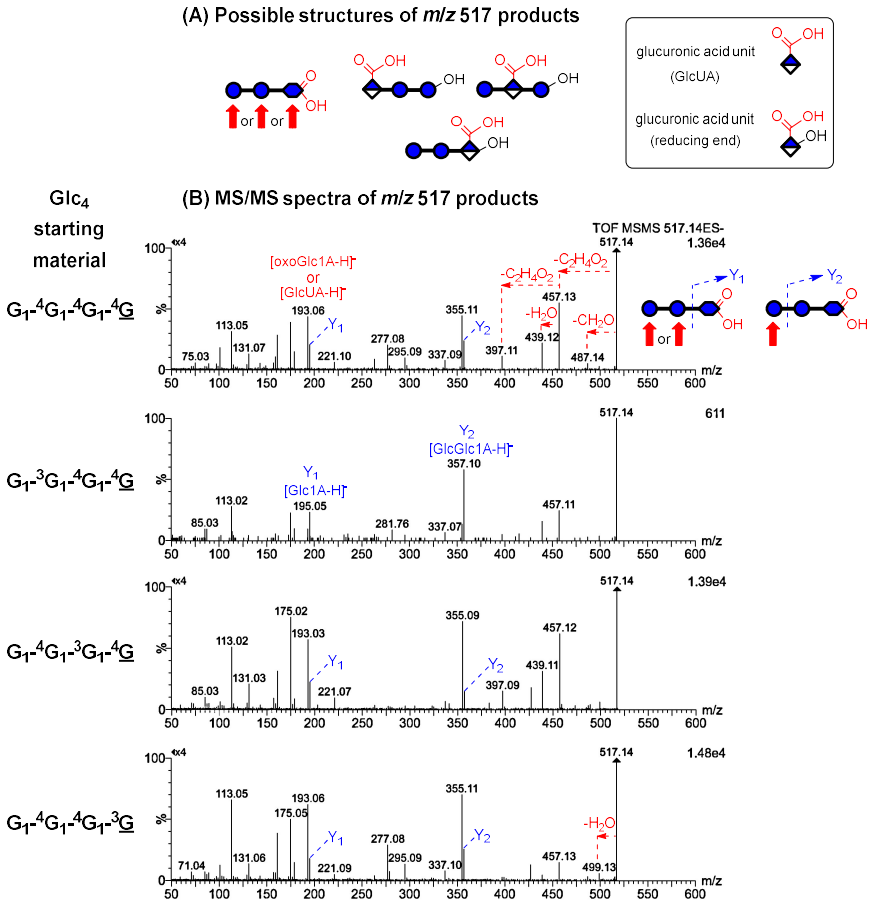

Fig. S13 (A) Possible acidic product structures with *m/z* 517 (oxoGlcGlcGlc1A and Glc_2GlcUA) shown in the case of cello-oligomers as example. The bold red arrows indicate possible positions of the carbonyl function on the oligomer with presumed gluconic acid end group. (B) Collective MS/MS spectra of *m/z* 517 products obtained from the various Glc_4 isomers under the Fenton conditions. Labelled Y_n fragments (blue) correspond to ions containing the gluconic acid unit, but not the additional carbonyl group, whereas neutral losses in red indicate oxo-product ions. ESI-method A.

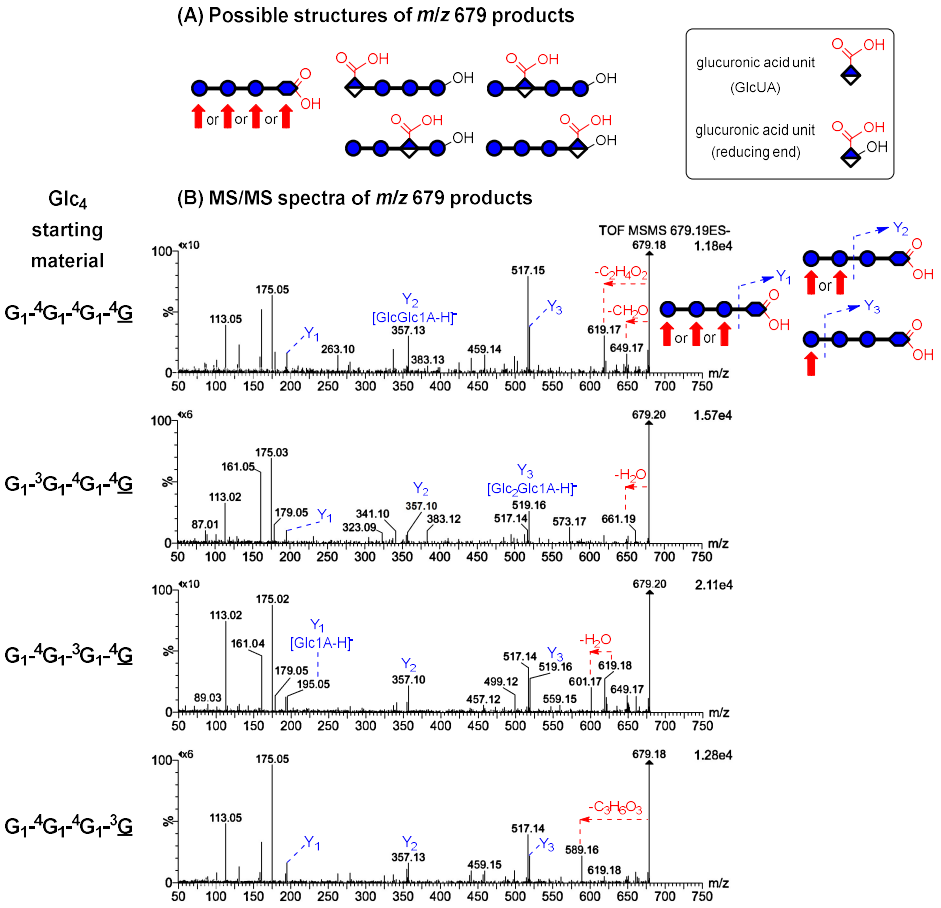

Fig. S14 (A) Possible acidic product structures with *m/z* 679 (oxoGlcGlc$_2$Glc1A and Glc$_3$GlcUA) shown in the case of cello-oligomers as example. The bold red arrows indicate possible positions of the carbonyl function on the oligomer with presumed gluconic acid end group. (B) Collective MS/MS spectra of *m/z* 679 products obtained from the various Glc$_4$ isomers under the Fenton conditions. Labelled Y_n fragments (blue) correspond to ions containing the gluconic acid unit, but not the additional carbonyl group, whereas neutral losses in red indicate oxo-product ions. ESI-method A.

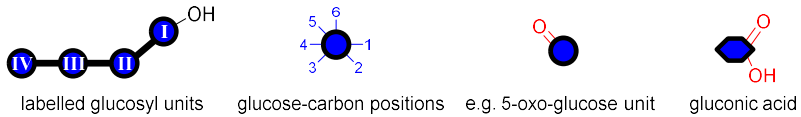

labelled glucosyl units | glucose-carbon positions | e.g. 5-oxo-glucose unit | gluconic acid

Table S5 Possible oxidation products depending on site of oxidative attack regarding glucose carbon and glucosyl unit on the oligomer with G_1-$^4G_1$-$^4G_1$-$^3\underline{G}$ (*m/z* 665) as example.[a]

Oxidation at carbon→	**C1**		**C2**	**C3**		**C4**		**C5**		**C6**
on glucosyl unit ↓	non-reducing end portion	reducing end portion	*(no cleavage)*	non-reducing end portion	reducing end portion	non-reducing end portion	reducing end portion	non-reducing end portion	reducing end portion	*(no cleavage)*
I	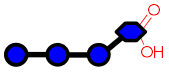 *m/z* 681		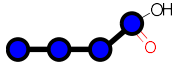 *m/z* 663	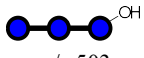 *m/z* 503	 *m/z* 177	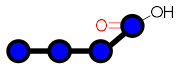 *m/z* 663		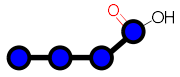 *m/z* 663		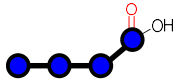 *m/z* 663
II	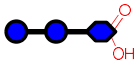 *m/z* 519	 *m/z* 179	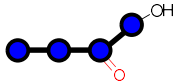 *m/z* 663	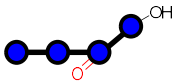 *m/z* 663		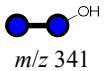 *m/z* 341	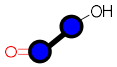 *m/z* 339	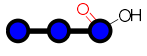 *m/z* 501	 *m/z* 179	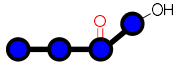 *m/z* 663
III	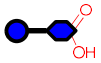 *m/z* 357	 *m/z* 341	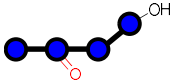 *m/z* 663	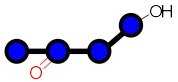 *m/z* 663		 *m/z* 179	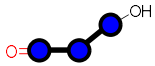 *m/z* 501	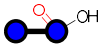 *m/z* 339	 *m/z* 341	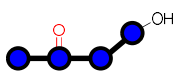 *m/z* 663
IV	 *m/z* 195	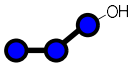 *m/z* 503	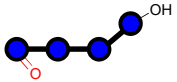 *m/z* 663	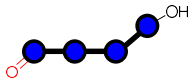 *m/z* 663		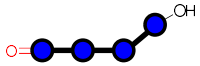 *m/z* 663		 *m/z* 177	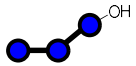 *m/z* 503	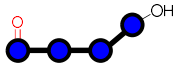 *m/z* 663

[a] Numbers under structures refer to *m/z* of $[M-H]^-$ species (for exact values see manuscript Table 1). Not that $HO^\bullet$ -attack at most of the glucose-carbons can alternatively also induce cross-ring scission. Here, only the most straight-forward direct oxidation products without loss of glucose-carbons are shown.

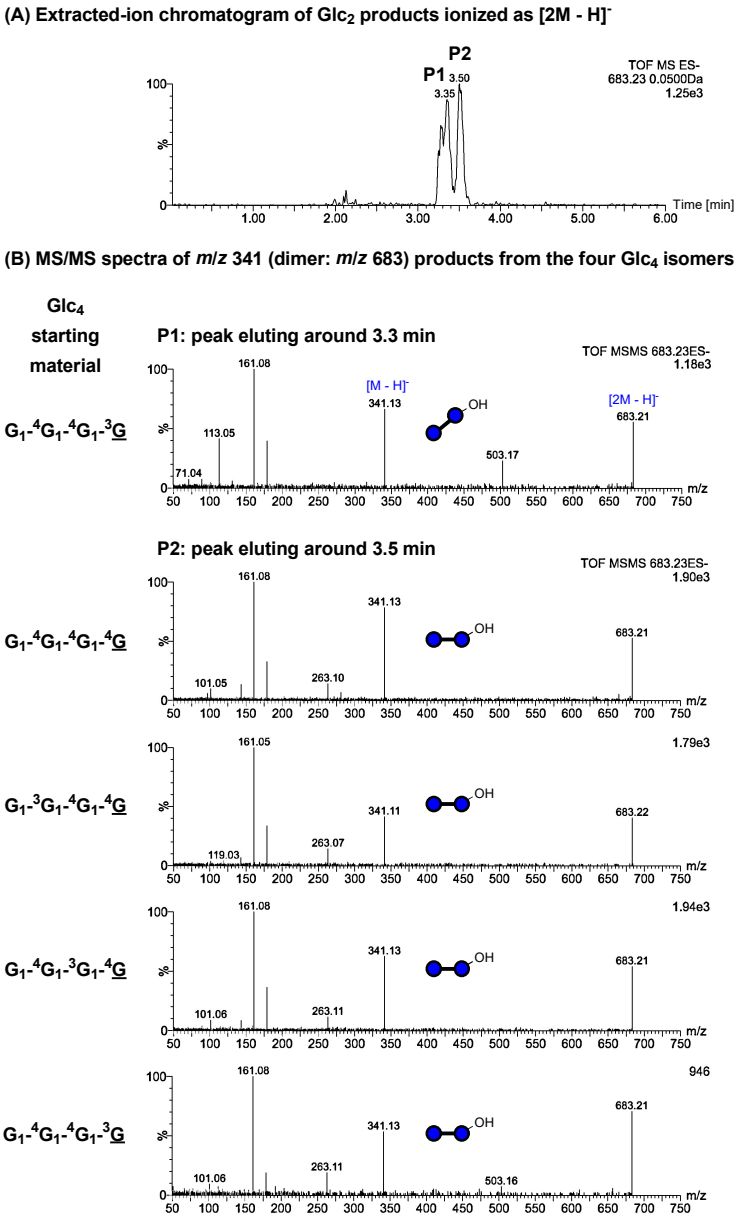

Fig. S15 (A) Extracted-ion chromatogram of the Glc_2 products ionized as $[2M - H]^-$ (*m/z* 683) from G_1-$^4G_1$-$^4G_1$-$^3\underline{G}$ degradation as example after 24 h (UPLC gradient 1; 0.1% NH_3 eluent; ESI-method A). Oxidation of the other three Glc_4 isomers produced only one peak at 3.5 min. (B) MS/MS spectra of two Glc_2 product peaks P1 and P2 from the degradation of four Glc_4 isomers with their respective product structures. Note that P1 was only observed with G_1-$^4G_1$-$^4G_1$-$^3\underline{G}$ as substrate.

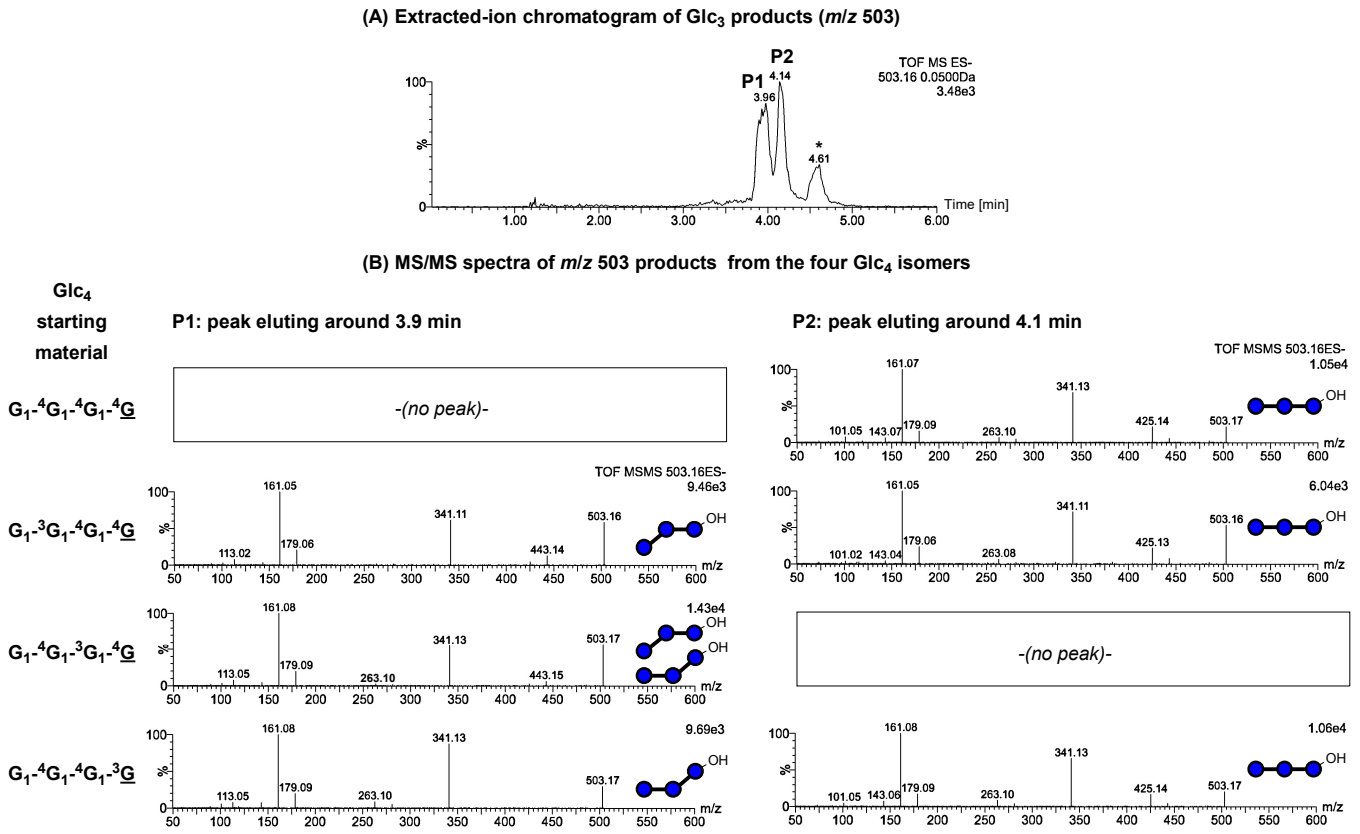

Fig. S16 (A) Extracted-ion chromatogram of the Glc_3 products (*m*/*z* 503) from G_1-$^4G_1$-$^4G_1$-$^3\underline{G}$ degradation as example after 24 h (UPLC gradient 1; 0.1% NH_3 eluent; ESI-method B). The peak labelled with an asterisk originates from the starting material Glc_4 eluting around 4.6 min and giving a signal with *m*/*z* 503 (C_3 ion) due to in-source fragmentation. (B) MS/MS spectra of two Glc_3 product peaks P1 and P2 from the degradation of four Glc_4 isomers. Note that the P1 product from G_1-$^4G_1$-$^3G_1$-$^4\underline{G}$ oxidation is a mixture of two mixed-linkage isomers which are not separable with the HILIC BEH Amide column, as the P1 MS/MS shows both fragments *m*/*z* 263 and 443, but with lower intensities than in the MS/MS of pure Glc_3 isomers G_1-$^4G_1$-$^3\underline{G}$ and G_1-$^3G_1$-$^4\underline{G}$ that each only show one of them.

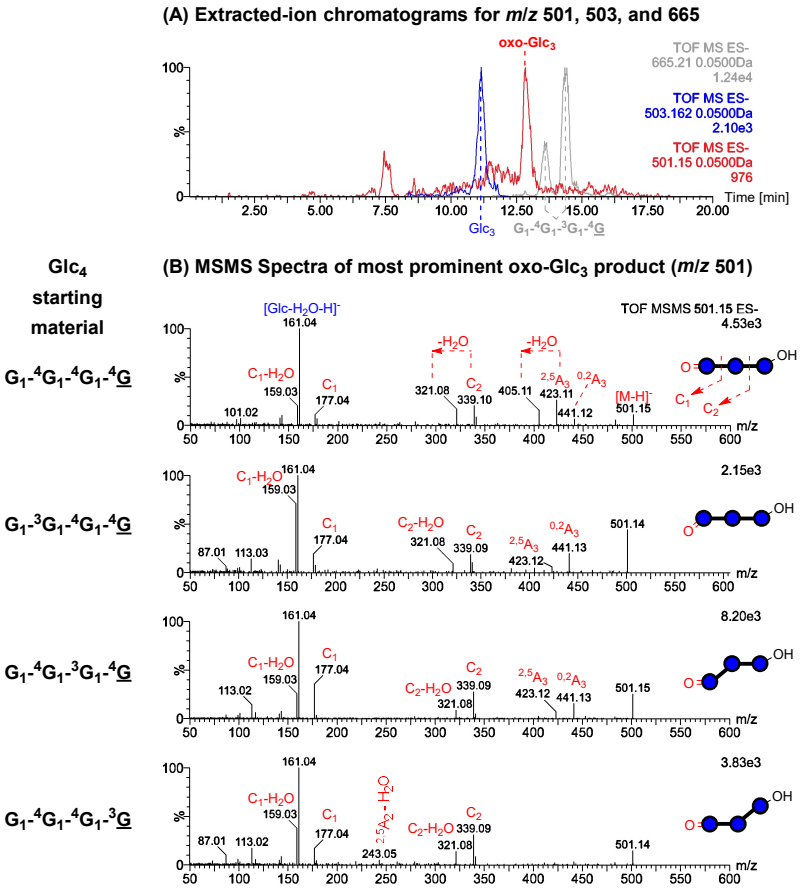

Fig. S17 (A) Extracted-ion chromatogram of the oxo-Glc_3 product (*m/z* 501, red) (and for comparison of retention times also of native Glc_3 product (*m/z* 503; blue) and remaining starting material Glc_4 (*m/z* 665; grey)) from G_1-$^4G_1$-$^3G_1$-$^4\underline{G}$ degradation as example after 12 h (UPLC gradient 2; 0.1% NH_3 eluent; ESI-method B). (B) MS/MS spectra of the most prominent oxo-Glc_3 product from the degradation of four Glc_4 isomers. The depicted product structures refer to the proposed main product isomers purely deduced from the fragmentation pattern (which confirms location of the carbonyl on the non-reducing end, but does not allow determination of its exact position on said unit. The carbonyl position is shown according to the lytic C3/C4 oxidation mechanism discussed in the paper). The fragment ions labelled in red refer to MS/MS fragments still bearing the additional keto-group.[vi]

[vi] Control experiments with base-treatment (pH ≥10) prior to injection confirmed that the observed species are <u>not</u> the isobaric lactone forms of the respective gluconic acids Glc_2Glc1A (no disappearance of peaks).

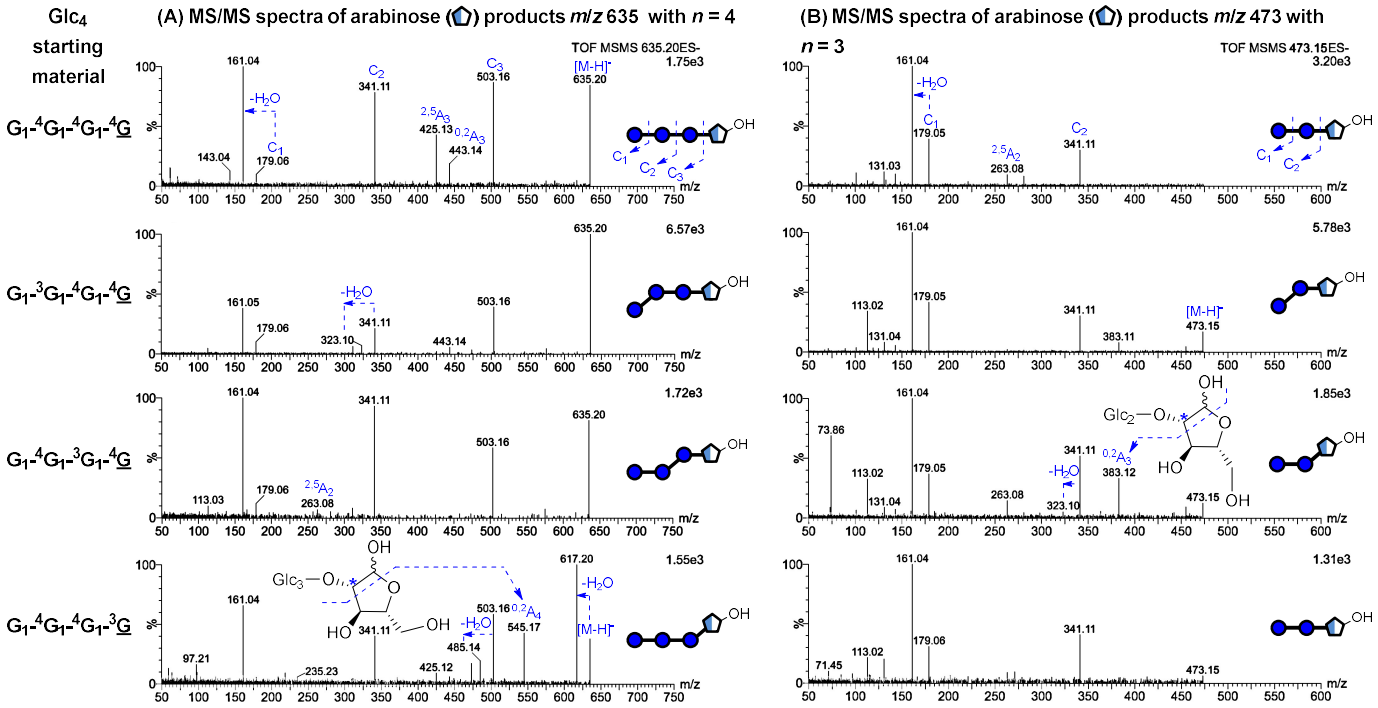

Fig. S18 MS/MS spectra of arabinose bearing oligomers $Glc_{(n-1)}Ara$ obtained from the various Glc_4 isomers under the Fenton conditions with (A) n = 4 and (B) n = 3. The depicted product structures refer to the main product isomer. The asterisk in the chemical structure indicates carbon 2 of arabinose (formerly glucose carbon 3). Note that the fragment $^{0,2}A_n$ is only possible with β-(1→2)-linked arabinose (formerly β-(1→3)-linked glucose), and is not observed with β-(1→3)-linked arabinose (formerly β-(1→4)-linked glucose). See paper for mechanistic reasoning of this type of retro-aldol fragmentation.

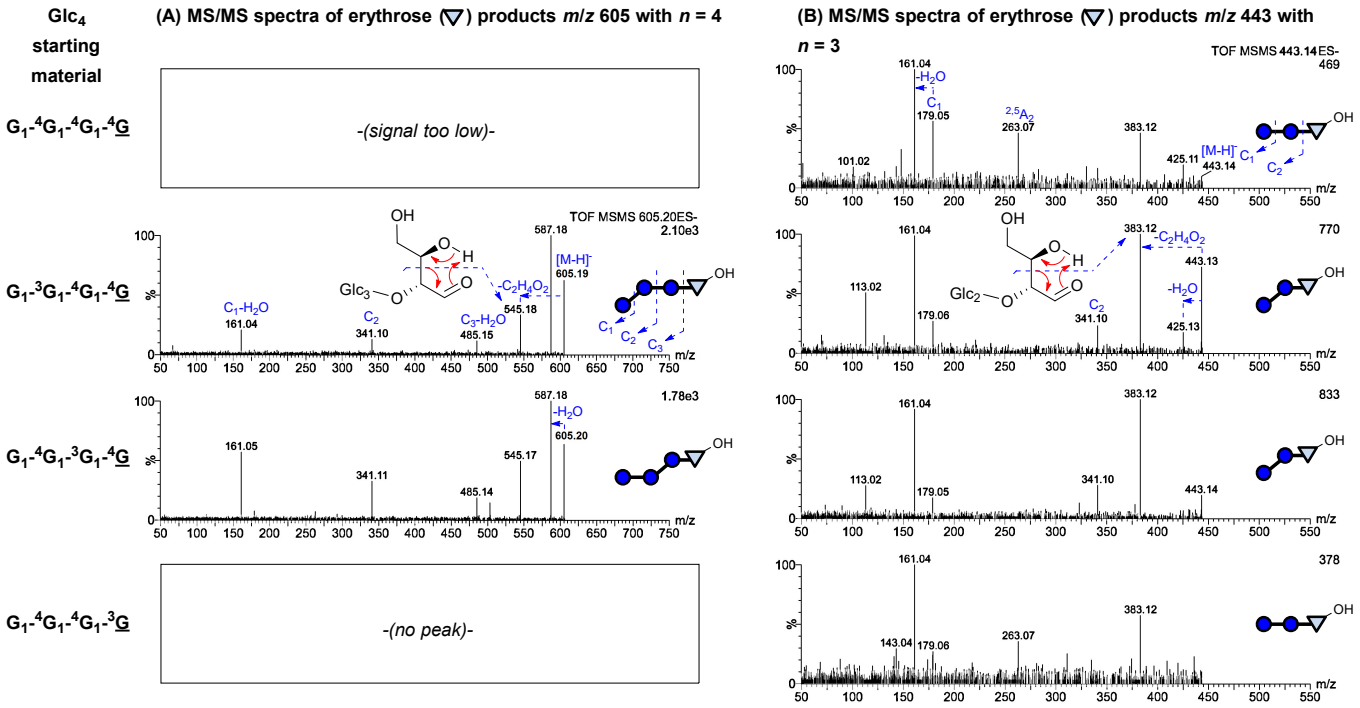

Fig. S19 MS/MS spectra of erythrose bearing oligomers $Glc_{(n-1)}Ery$ obtained from the various Glc_4 isomers under the Fenton conditions with (A) n = 4 and (B) n = 3. The depicted product structures refer to the main product isomer. The two chemical structures show the retro-aldol reaction to fragment m/z 545 and 383 for n = 4 and n = 3, respectively. Note that the m/z 605 product from G_1-$^4G_1$-$^4G_1$-$^3\underline{G}$ is not possible (required loss of carbon to produce erythrose end group is linked to Glc_3) and was not observed. The m/z 443 product from G_1-$^4G_1$-$^3G_1$-$^4\underline{G}$, on the other hand, gave an isomer consistent with secondary oxidation of a released G_1-$^3G_1$-$^4\underline{G}$.

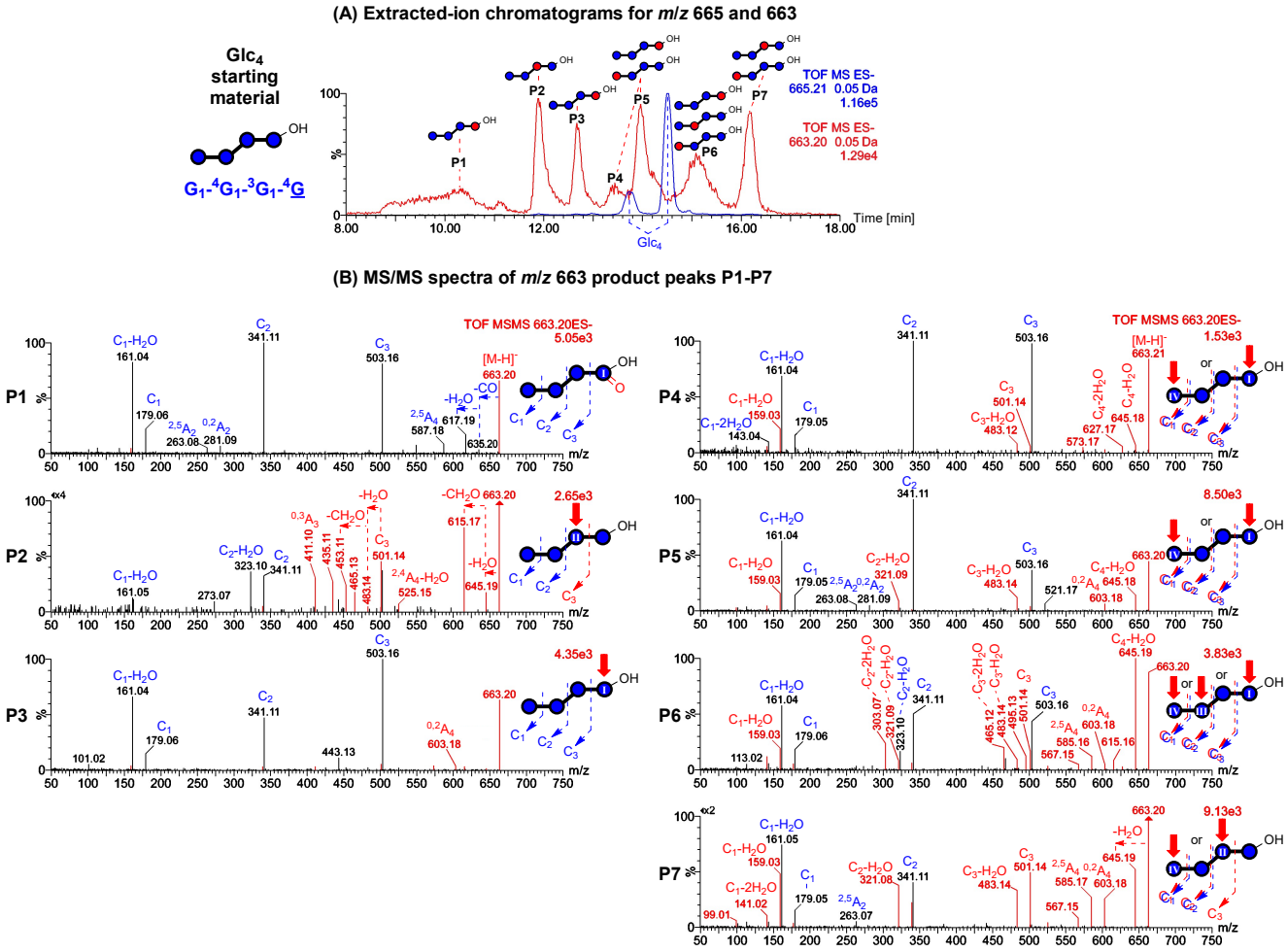

Fig. S20 (A) Overlaid extracted-ion chromatograms (UPLC gradient 2; 0.1% NH_3 eluent; ESI-method B) of the starting material Glc_4 (m/z 665, blue) and the oxo-Glc_4 products (m/z 663, red) from G_1-$^4G_1$-$^3G_1$-$^4\underline{G}$ degradation. The depicted structures above the peaks represent the tentatively proposed main components of each peak as determined by MS/MS (oxo-glucosyl units in red). (B) MS/MS spectra of all seven oxo-Glc_4 peaks. The bold red arrows indicate where oxidation mainly occurred in the mixture of products. Red and blue signals/ labels in the MS spectra refer to fragments with and without the additional carbonyl group, respectively. The spectra on the left (P1–3) refer to product mixtures that do not contain the carbonyl group at the non-reducing end (IV), while the ones on the right (P4–7) do.[vii]

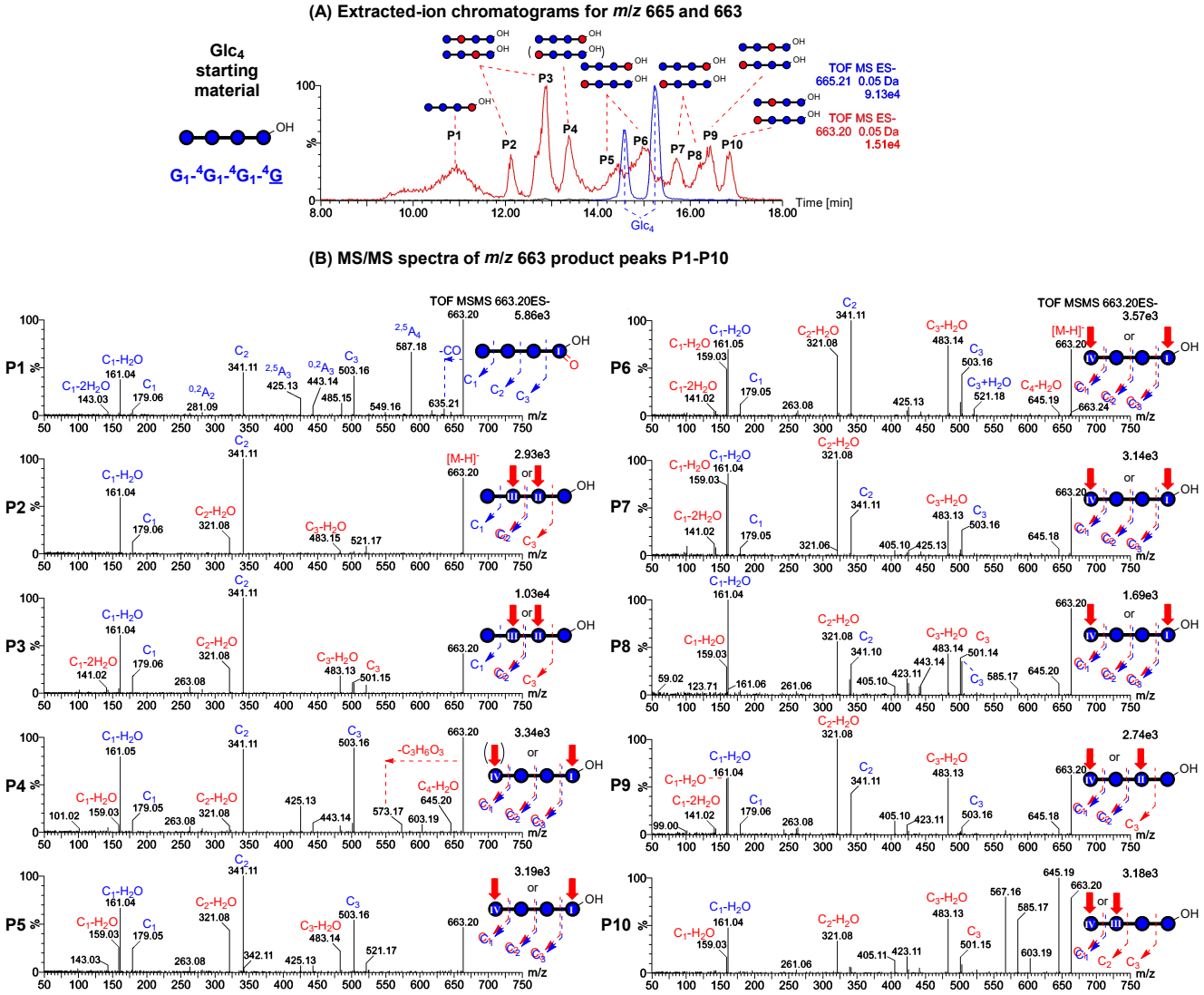

Fig. S21 (A) Overlaid extracted-ion chromatograms (UPLC gradient 2; 0.1% NH_3 eluent; ESI-method B) of the starting material Glc4 (m/z 665, blue) and the oxo-Glc4 products (m/z 663, red) from G_1-$^4G_1$-$^4G_1$-$^4\underline{G}$ degradation. The depicted structures above the peaks represent the tentatively proposed main components of each peak as determined by MS/MS (oxo-glucosyl units in red). (B) MS/MS spectra of all ten oxo-Glc4 peaks. The bold red arrows indicate where oxidation mainly occurred in the mixture of products. Red and blue labels in the MS spectra refer to fragments with and without the additional carbonyl group, respectively.[vii]

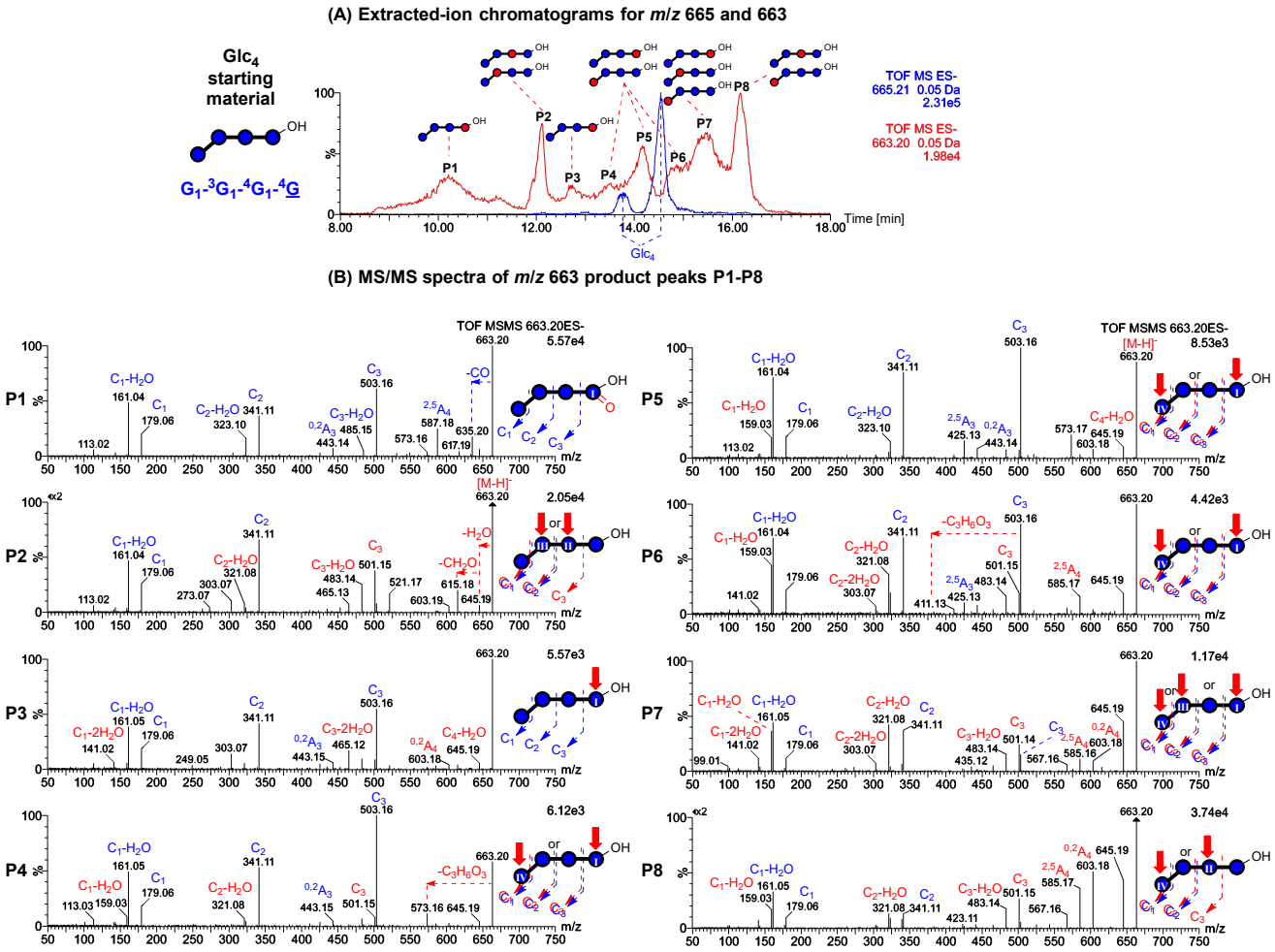

Fig. S22 (A) Overlaid extracted-ion chromatograms (UPLC gradient 2; 0.1% NH_3 eluent; ESI-method B) of the starting material Glc_4 (m/z 665, blue) and the oxo-Glc_4 products (m/z 663, red) from G_1-$^3G_1$-$^4G_1$-$^4\underline{G}$ degradation. The depicted structures above the peaks represent the tentatively proposed main components of each peak as determined by MS/MS (oxo-glucosyl units in red). (B) MS/MS spectra of all eight oxo-Glc_4 peaks. The bold red arrows indicate where oxidation mainly occurred in the mixture of products. Red and blue labels in the MS spectra refer to fragments with and without the additional carbonyl group, respectively.[vii]

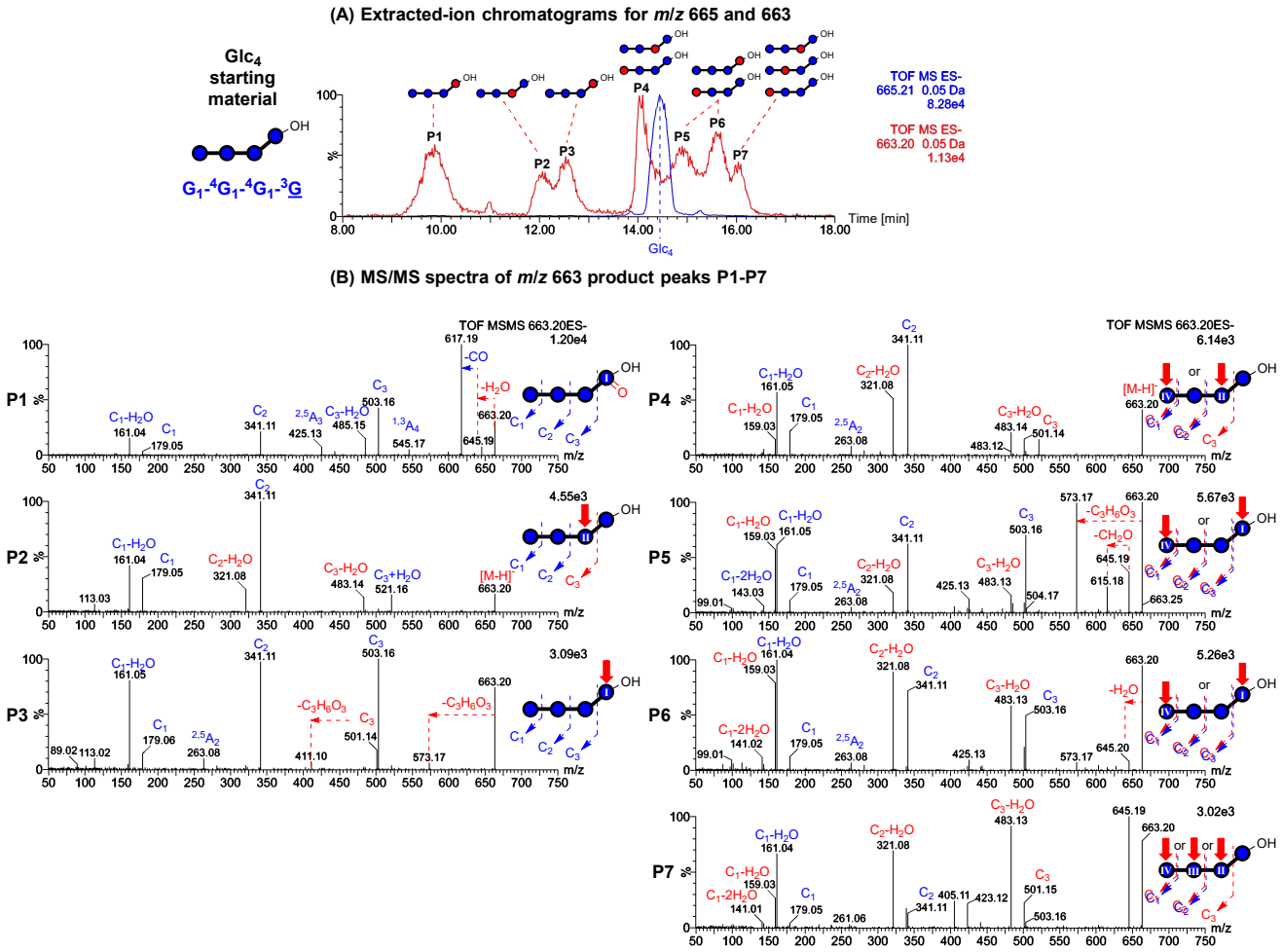

Fig. S23 (A) Overlaid extracted-ion chromatograms (UPLC gradient 2; 0.1% NH_3 eluent; ESI-method B) of the starting material Glc_4 (m/z 665, blue) and the oxo-Glc_4 products (m/z 663, red) from G_1-$^4G_1$-$^4G_1$-$^3\underline{G}$ degradation. The depicted structures above the peaks represent the tentatively proposed main components of each peak as determined by MS/MS (oxo-glucosyl units in red). (B) MS/MS spectra of all seven oxo-Glc_4 peaks. The bold red arrows indicate where oxidation mainly occurred in the mixture of products. Red and blue labels in the MS spectra refer to fragments with and without the additional carbonyl group, respectively.[vii]

[vii] Control experiments with base-treatment (pH ≥10) prior to injection confirmed that <u>none</u> of the observed species are the isobaric lactone forms of the respective gluconic acids Glc_3Glc1A (no disappearance of peaks). Note that some products might elute as two peaks (α/β-anomers), and that the carbonyl location is not unambiguously assignable for mixtures that also contain oxidation at the internal units (II & III). Hence, mixtures that contain both products with oxidation at the termini (I & IV) could also contain products with the carbonyl at the internal units (II & III).